Fizika Nizkikh Temperatur, 2003, v. 29, No. 6, p. 699–705

Quench deposited $Kr–H_2$ and $Ar–H_2$ mixtures: in quest of impurity-hydrogen gels

M.A. Strzhemechny, N.N. Galtsov, and A.I. Prokhvatilov

B. Verkin Institute for Low Temperature Physics and Engineering of the National Academy of Sciences of Ukraine, 47 Lenin Ave., Kharkov 61103, Ukraine
E-mail: galtsov@ilt.kharkov.ua

Received December 19, 2002

The structure and morphology of low-temperature quench condensed binary alloys of hydrogen with argon and krypton were studied by the powder x-ray diffraction. The nominal hydrogen fraction c in both systems was varied from 0 to 50%; the condensation was performed at 5–6 K; both as-prepared and annealed samples were examined by the x-ray diffraction. Few, often only one reflection can be unambiguously detected for the as-grown alloy samples. In the $Kr–H_2$ condensates with $c < 10\%$, the x-ray patterns show fine-grain krypton-rich crystallites with rather high actual hydrogen contents as estimated from Vegard's law. At high nominal hydrogen fractions ($c \geq 10\%$), no the reflections attributable to the krypton lattice were recorded and the incoherent background showed no characteristic swelling around the position of reflection (111) from pure Kr but, instead, the reflections from a hydrogen-rich hcp phase were distinct. As the temperature was steadily raised, first the hydrogen reflections disappeared and then, at a certain temperature, the samples underwent an abrupt transformation, releasing heat and making the krypton component forms larger, x-ray detectable textured crystallites. In the as-grown $Ar–H_2$ samples, only (111) reflections from the argon-rich phase were recorded. Warmup led to the same consequences, viz., effusion of hydrogen and then recrystallization. In both systems, the recrystallization onset temperature depends substantially on the nominal hydrogen fraction in the gas. The shift of the lattice parameter in the as-grown argon-based phases suggests a strong suppression of the quantum nature of hydrogen in argon lattice environment. The entire set of the experimental findings can be treated as evidence that the quench-condensed hydrogen-containing alloys morphologically resemble helium–impurity solids (gels) whose structure and morphology are currently studied at Cornell University.

PACS: **61.10.–i**, 61.43.Dq, **61.66.–f**

1. Introduction

Binary systems like mixtures of hydrogen and rare gas (RG) species are interesting for solid state physics because the relative simplicity of the basic interactions involved enable an unambiguous interpretation of the phenomena observed. Because of the large mismatch in the molecular parameters σ and ε of hydrogen and the heavier rare gas atoms, one could hardly expect at low pressures an appreciable equilibrium solubility in the solid of these mixtures at both ends of the fraction range. Only application of a considerably pressure makes some of these mixtures form stoichiometric compounds like $Ar(H_2)_2$ [1] or a series of such compounds in hydrogen–methane mixtures [2]. There are other high-pressure hydrogen-based compounds (cf. Schouten's review [3]). The low mutual miscibility of hydrogen with the heavier rare gas species might be helpful in producing hydrogen-based self-sustained condensed media. This idea with ^{4}He as the main binding material was first suggested [4] and subsequently implemented [5] in Chernogolovka, Russia. The preparation technique consists in blowing a jet of the species chosen into superfluid ^{4}He. The pivotal factor is the extremely high thermal conductivity of superfluid helium, which enables momentary dissipation of the energy coming with the particles in the jet. Later these helium–impurity solids with different impurities were extensively studied by Gordon's group (for references see Ref. 6). Later studies at Cornell [7–9] led to the conclusion that these materials are highly porous amorphous media made up of particles or small clusters surrounded by layers of helium,

which could be considered solidified due to the external forces of the impurity–helium interactions. Since hydrogen cannot guarantee a heat removal like in superfluid ^{4}He, in order to get a hydrogen–impurity solid it seems worthwhile to try quench condensation of the corresponding mixture at high deposition rates. So, one of the basic motivations was to look for possible highly amorphized states in both systems. Proceeding from the known mismatch of the molecular parameters of the heavier rare gas atoms and hydrogen we expected to obtain condensates that would have properties resembling those of impurity–helium solids (gels).

Apart from this principal aim, our motivation was also to elucidate the structural consequences of admixing heavy RG species to hydrogen and quench condensing the mix. It is important for a few reasons. It was mostly interesting to try to determine the equilibrium miscibility edge at the RG side, which is important for the purposes of low temperature thermodynamic investigations on dilutions of various molecular species in solid hydrogen (cf. an overview in the book by Manzhelii et al. [10]).

In this paper we report results of powder x-ray studies on the Ar–H_2 and Kr–H_2 binary systems in the concentration range of mixtures rich in the rare gas elements. Special attention was paid to the structure and phase state of the samples and the effect of deposition rates of the gas mixes. These results are analyzed in the light of possible hydrogen–impurity solids (gels).

2. Experimental

These structure studies were performed on a x-ray diffractometer DRON-3M equipped with a liquid-helium cryostat. Radiation Fe K_α was used. Diffractometer control, data collection and processing were accomplished from PC. Samples were produced by condensing gas mixtures of known compositions directly into the solid phase onto a flat copper substrate at a temperature of 5 or 6 K. This procedure allowed us to suppress the natural tendency of hydrogen to grow in large-size single crystals and, instead, to obtain 0.1 mm thick polycrystal samples with coherent scattering area sizes of order 10^{-4}–10^{-5} cm. The purity of the gases for H_2, Ar, and Kr was 99.99%. The fraction of normal hydrogen in the gaseous Ar–H_2 and Kr–H_2 mixes was varied from 1 to 50%. The relative error in the composition of the binary gas mixtures did not exceed 5% with respect to the amount of hydrogen introduced.

The sample preparation procedures employed in this investigation was based on our experience of working with solid hydrogen [11] as well as hydrogen doped with neon [12] and some other simple molecules [13]. Growth of condensates was performed using two deposition regimes, which differed in the amount of material in a single gas deposition burst. In one of the regimes, every deposition step resulted in a 3 to 4 Torr drop of the pressure inside the gas mixing chamber; during the other regime the pressure drop was typically twice as large. In order to avoid selective freeze-out of the less volatile rare gas component from the gas mix on its way from chamber to substrate, the temperature of the filling duct was maintained at a sufficiently high level, close to room temperature. To this end, the thin-walled stainless steel filling capillary was connected to the cooling chamber through a Teflon capillary.

The samples were x-ray diffraction examined at once after deposition and subsequently on warmup in a step-like manner (every 5 or 10 K) up to 50 K. At every working point the temperature was stabilized to within ±0.05 K. Because of the small number of recordable reflections and overlap of separate reflections from different phases, the error in the lattice parameter determination was noticeably larger than typical of x-ray studies of pure cryocrystals but did not exceed ±0.05%.

3. Results and discussions

One of the main goals of this work was to determine the structure state of as-grown samples and, when possible, to evaluate the limiting solubility of hydrogen in the two rare gas solids under the condensation conditions specified above. The structure of freshly grown samples differed substantially for different nominal hydrogen contents c in the gas mixture.

Krypton

In experiments with elevated (c = 10 to 40%) hydrogen contents we obtained patterns with rather unexpected properties. First, all as-grown samples deposited on the 5 K substrate did not produce reflections characteristic of the krypton lattice. Second, incoherent background did not contain smeared maxima (diffuse halo), typical of the systems with well formed short-range order. Third, in spite of the lower fraction of hydrogen in the mix, we saw distinct reflections from a crystal phase that could be attributed to the hydrogen crystal, possibly with a certain nonzero krypton content (Fig. 1). The essential qualitative changes in diffraction patterns between 4 and 10% gave us ground to infer that the samples with nominal hydrogen content of 10% and higher have an unusual morphology. By all appearances, the krypton-rich phase in those as-grown samples was in an amorphous or/and highly finely disperse state, while part of the hydrogen fraction with a relatively low krypton content was crystallized

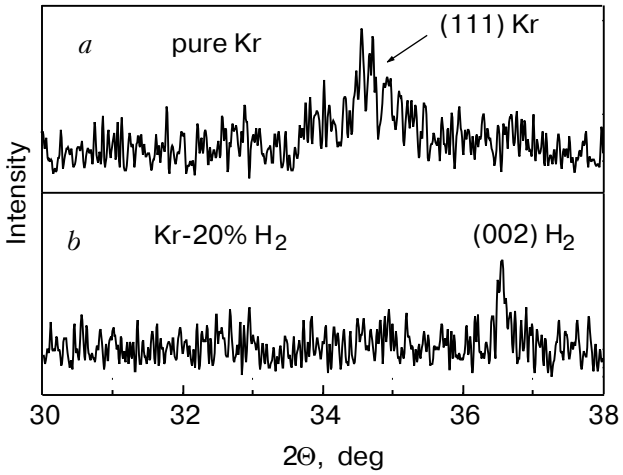

Fig. 1. Fragments of powder x-ray patterns from pure krypton (*a*) and a $Kr-20\%H_2$ alloy (*b*), both obtained by quench deposition from the gas on a flat copper substrate at T = 5 K. The arrows indicate the reflections from the respective crystal planes. Note absence of Kr reflections from the hydrogen-doped as-grown sample.

into a fine-grained textured phase, which was recordable by x-rays. The hydrogen-rich phase observed within the range of nominal concentrations 10–40% was nonstrained and structurally perfect; reflection (002) had a small width of 0.1–0.15 degrees. Variations of the deposition rate did not affect the sample's parameters. By applying the straightforward Vegard law, i.e., making use of the cube root of the molar volumes of pure krypton and hydrogen, we estimated the actual krypton concentration x_{Kr} in hcp H_2 as being around 4%. It should be added here that the angular position of mixed crystals depends not only on the impurity concentration but also on the density of stacking faults α, amount of which might be rather high, especially in freshly grown samples. It is quite safe to evaluate the impurity concentration using the (002) reflection of a hcp structure, because the position of precisely this reflection is not affected by stacking faults [14]. As to the fcc reflection (111), which we have at our disposal for the Kr-rich phases, it shifts to higher angles owing to stacking faults [14]. The reflection (111) from pure quench condensed krypton in Fig. 1 is appreciably shifted to larger angles. Taking this shift as being due to stacking faults we find [14] that α corresponds to an average number of planes between faults equal to 11 ± 3, which is a very high density but fairly consistent with the reflection width and intensity. The strong effect of stacking faults on the position of reflection (111) makes the estimation of the actual hydrogen concentration uncertain with a tendency for underestimation because both factors (impurities and faults) shift the (111) line to higher angles.

There is also another consideration that should be taken into account, when using Vegard's law in estimations of the actual H_2 content in Kr. As it will be proven below, when H_2 is dissolved in the argon lattice, the quantum nature of hydrogen molecules is considerably suppressed. Although we do not have direct unambiguous evidence for Kr-based mixtures, it seems quite reasonable to assume that this consideration is applicable for the Kr matrix as well. If the zero-point motion of the hydrogen molecules is ignored, then the lattice parameter appearing in Vegard's law should be calculated not from the actual molar of H_2 but [15] rather from the value σ^3, where σ = = 2.96 Å is the van der Waals radius of the hydrogen molecule.

When the samples with high nominal hydrogen content were warmed up to 14 K or higher, the reflection from the hydrogen phase disappeared (compare curves *a* and *b* in Fig. 2). When the temperature was increased to 30 K, a very broad and weak reflection, attributable as (111) of a krypton-rich phase, appeared (curve *c*). As the temperature was further raised, the reflection grew in intensity and narrowed (curve *d*). It can be surmised that within this temperature range, effusion of hydrogen from krypton started. At a certain temperature T_s an abrupt annealing and (re)crystallization occurred, which manifested itself in much higher intensities and smaller widths of the reflection.

Traces *b*, *c*, and *d* in Fig. 2 can be utilized to evaluate the actual concentration x_H in the Kr-rich phase at higher temperatures. Here we must take into account the numerous stacking faults inevitably present in the sample. If we assume their density to be the same $\alpha \simeq 1/11$ as found in the quench condensed sample of Fig. 1, we evaluate x_H to be $(3.8 \pm 0.4)\%$

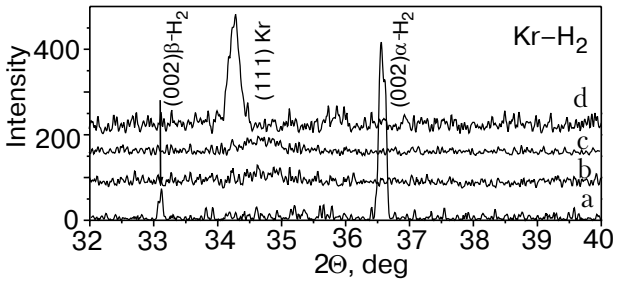

Fig. 2. Effect of warmup on the structural state of a $Kr-30\%H_2$ alloy, quench deposited at T = 5 K. All patterns were recorded without filter to see more clearly the evolution of the sample. Pattern (*a*) is from the sample freshly quench deposited on 5 K; only the (002) reflection from the basal plane of the hexagonal hydrogen-rich lattice can be seen; a K_β reflection from the hydrogen is seen at smaller angles. Patterns (*b*) through (*d*) correspond to annealing temperatures, respectively, 35, 43, and 48 K.

at 35 K and (3.5 ± 0.5)% at 43 K. (We made use of the lattice parameters measured for pure Kr at different temperatures by Losee and Simmons [16].) After the quick recrystallization is over (trace *d*), one can expect the sample to be virtually free of hydrogen. Indeed, the position of line (111) coincides within the aggregate error with the value for pure Kr at the same temperature, which implies that the stacking-fault and impurity concentrations are close to zero.

At lower nominal hydrogen fractions ($c < 10\%$) we saw only reflections that could be attributed to line (111) from a cubic krypton-rich lattice with a somewhat smaller lattice parameter than in pure krypton. Within a rather large uncertainty the respective lattice parameter shifts for c = 1, 2, and 5% may be considered constant and corresponding to the absolute lattice instability edge. If uncorrected Vegard's law is applied, we obtain an appreciable hydrogen concentration x (H_2 in Kr) = (1.4 ± 0.3) %, the presence of hydrogen manifesting itself in a slight lattice constriction. However, it should be born in mind that this estimate does not account for stacking faults. The reflections observed were the more intensive the lower the nominal hydrogen fraction. Irrespective of the condensation rate the reflections were broadened, which suggests small grain sizes and a high concentration of lattice defects.

Effect of the gas deposition rate mainly manifested itself in variations of the temperatures T_s where recrystallization and annealing of amorphous specimens occurred. A general trend was that the crystallization temperature somewhat increased at higher condensation rates. Thus, for the low-rate condensation regime, crystallization of the apparently amorphous Kr–20%H_2 condensate was observed at a temperature of 35 K. Under the twice as fast deposition rate, crystallization began at around 40 K.

A more pronounced dependence of the crystallization starting temperature for krypton-based mixtures was observed with varying composition of the source mixes (Fig. 3). Samples with 10 to 25% H_2 began to recrystallize at 35–40 K. The crystal phase in recrystallized samples was strained and imperfect, which was inferred from broad and low-intensity reflections. Keeping the samples for 5 hours even at the crystallization onset temperature resulted in a complete recrystallization, the intensity and width of the Kr reflections approaching the values observed previously for pure krypton. A slight temperature increase resulted in quickening the process considerably. Samples with the nominal hydrogen content ranging from 30 to 40% underwent recrystallization at higher temperatures in the range 45–55 K (Fig. 3). One can see that the curve for the Kr–H_2 system has a kink at lower c values, which might reflect the basic differences in structure and morphology between samples grown from hydrogen-dilute and hydrogen-concentrated gas mixes. The distinct shift of the crystallization onset temperature to higher values at higher nominal hydrogen fractions indicates that hydrogen tends to stabilize the unusual amorphous krypton phase in as-grown samples.

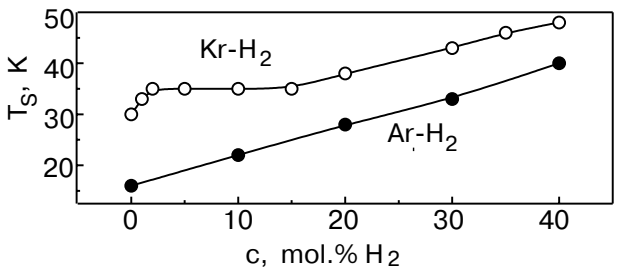

Fig. 3. The annealing onset temperatures of Kr–H_2 (○) and Ar–H_2 (●) alloys as a function of the nominal hydrogen fraction in the source gas mix.

The latest results of the Cornell group [9,18] show that morphologically the so-called impurity–helium solids are highly amorphous media in which the impurities form a multi-connected network of separate atom, *n*-mers, chains, nano-particles, etc., isolated from one another by layers of helium, presumably in the solid state. Basically, the impurity system can be treated as a non-self-sustained gel, which is stabilized at low enough temperatures by the helium spacer layers. As the sample is warmed up, the impurity fraction starts to coalesce and the latent heat makes helium atoms effuse, causing a burst-like reorganization of the matter. In many aspects, the hydrogen-containing krypton-based mixtures studied in this work resemble the impurity–helium media. There are a few pieces of evidence that confirm this assumption, namely, the highly amorphous state of the krypton-rich phase; the strong dependence of the crystallization onset temperature T_s on the nominal and, presumably, actual hydrogen concentrations; the very existence of T_s at which a sample undergoes a cardinal and fast reconstruction. What can be said for sure is that hydrogen is a factor that stabilizes those amorphous states.

In Fig. 4 we plot the lattice parameters a of the samples after annealing as a function of the nominal hydrogen fraction c in the gas mix. All a values were determined at 5 K. The «final» a is virtually independent of c. Assuming no stacking faults and using corrected Vegard's law (dotted line), we evaluate the actual hydrogen concentration x_H to be close to 1% (use of uncorrected Vegard's law yields 4%). This figure should be treated as the ultimate estimate for the equilibrium solubility of H_2 in solid crystalline krypton.

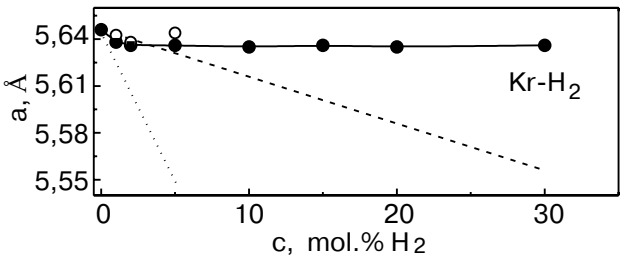

Fig. 4. The cubic lattice parameter of the krypton-rich phases in $Kr–H_2$ mixtures *versus* the nominal hydrogen fraction in the source gas (empty and solid circles are respectively for as-grown and completely annealed samples). The long-dash curve shows uncorrected Vegard's law for this system. The dotted curve is corrected Vegard's law (for explanation see the argon subsection in Sec.3).

Argon

The structural characteristics of as-grown $Ar–H_2$ condensates differ considerably from those observed on $Kr–H_2$ condensates. There was an important peculiarity, namely, the brightest reflections (111) from the Ar cubic phase and (002) from the hexagonal H_2 phase overlap, which makes reflection identification difficult. Use of other reflections was impossible because they were, as in the $Kr–H_2$ system, absent, which might be indicative of a texture even in very fine-grained samples. Therefore, some conclusions for the $Ar–H_2$ system are less reliable compared to the $Kr–H_2$ system.

The following findings should be noted for the $Ar–H_2$ mixtures. First, irrespective of the growth regime, within the entire range of nominal hydrogen concentrations up to $c = 50\%$ the mixed samples gave reflections that were broader and less bright as compared to that from pure solid argon prepared under similar deposition conditions (Fig. 5). Pure argon was easily annealed at a comparatively low temperature around 16 K. The annealing onset temperature increased almost linearly with increasing c, remaining however always lower than for the $Kr–H_2$ system (Fig. 3).

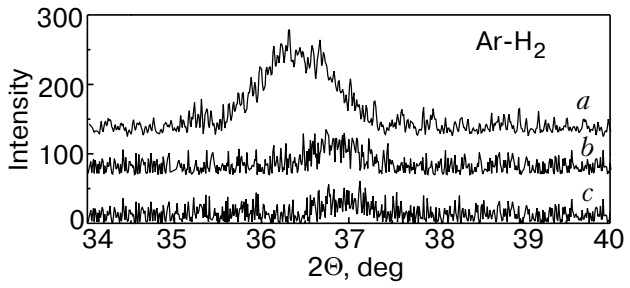

Fig. 5. Effect of hydrogen impurities on the angular position and intensity of the (111) reflection from quench grown $Ar–H_2$ samples: pure argon (*a*); condensates with nominal hydrogen fractions of 10% (*b*) and 30% (*c*).

Second, although the assignment of the only recordable reflection was dubious (Gaussian deconvolution always gave only one line), judging from its position and the general behavior with temperature, we attributed this reflection as the (111) line from the argon-rich fraction. Over the entire nominal H_2 concentration range we did not identify reflections from the hydrogen-rich phase, either upon condensation or after annealing during 1 hour at 10–12 K.

The above findings allow us to conclude the following. Since it is unlikely that hydrogen formed a superfine-grain phase, we surmise that H_2 entered completely into the argon lattice as well as the hydrogen-argon gel, existence of which cannot be ruled out. The following facts favor this assumption: 1) reflections from as-grown condensates are weaker and broader compared to those from pure as-grown samples; 2) reflections from the argon-rich phase are substantially shifted to larger angles compared to pure argon; 3) a considerable increase of the recrystallization onset temperature with increasing nominal hydrogen fraction was observed. At the same time, annealing of the samples resulted not only in larger intensities and smaller widths of the reflection but also in substantial shift to smaller angles, i.e., in larger lattice parameters of the argon lattice closer to the values typical of pure crystalline argon. Effect of annealing on the intensities and line widths of the argon matrix is clearly demonstrated in Fig. 6. Annealing at $T > 20$ K resulted in brighter and narrower reflections from plane (111) of the argon matrix. A shift of this line to smaller angles is distinctly seen, which again means an increase in lattice parameter. Figure 7 shows effect of hydrogen impurities on the cubic lattice parameter a of the Ar matrix in as-grown and annealed samples. The unusual finding is that a in as-grown argon-based phase, where a finite concentration of hydrogen is expected, is *smaller* than in annealed samples, which are presumably devoid of hydrogen impurities, opposite to what can be expected from a straightforward Vegard

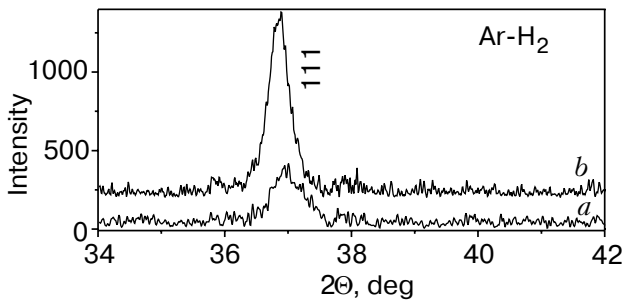

Fig. 6. Effect of annealing on the intensity and half-width of reflection (111) in the $Ar–H_2$ system. Trace (*a*) is from an as-grown $Ar–20\%H_2$ condensate; trace (*b*) is from the same sample upon annealing.

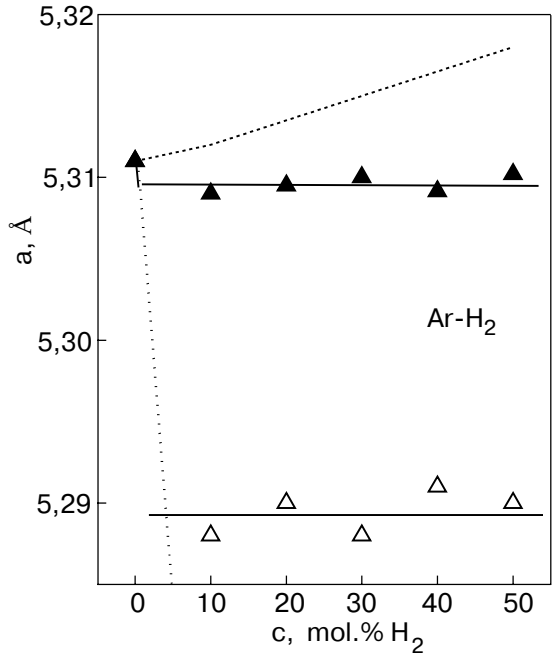

Fig. 7. The cubic lattice parameter of the krypton-rich phases in $Ar–H_2$ mixtures *versus* the nominal hydrogen fraction in the source gas for freshly deposited specimens (△); annealed specimens (▲). The dashed curve shows uncorrected Vegard's law for this system; the dotted curve is corrected Vegard's law (for explanation see the argon subsection in Sec.3).

line, which must have a positive, however small, slope. This fact suggests the following reasoning. The intermolecular spacing in pure hydrogen is governed by an effective potential, renormalized considerably to account for large zero-point vibrations. If a hydrogen molecule is placed in the argon lattice, one can expect that due to much stronger interactions with the argon environment the quantum nature of the H_2 molecule will be substantially suppressed. If this suppression is ultimate, then the intermolecular distance used in Vegard law estimates should be close to the hydrogen van der Waals diameter σ, as is the case with any «classical» heavy particle. That is, the effective hydrogen molar volume to be used in Vegard law calculations at the argon side of the (a, x) phase diagram should be [15] σ^3. The Vegard line corrected in that way is shown in Fig. 7 as the (relatively) steep line with negative slope. Using now the corrected Vegard law, we estimate that the hydrogen concentration in as-grown argon-based phase to be 3.6%. Account of stacking faults inevitably present in as-grown samples must reduce this estimate at least twice. The corrected actual hydrogen concentration (1 or 2 %) in as-grown samples and the still smaller value in annealed samples (see Fig. 7) compares well with the upper estimate for the solubility of hydrogen in solid argon of 0.5 mol% found by Loubeyre et al. [1].

4. Conclusions

1. When room-temperature $Kr–H_2$ and $Ar–H_2$ gas mixtures are quench condensed on a substrate at 5 K, the condensates tend to grow as highly amorphized structures. This is in particularly true for Kr-based samples with nominal hydrogen fractions above 10%, when as-grown samples did not give at all reflections that could be attributed to a krypton-rich phase.

2. When quench condensed samples were warmed up, the recrystallization onset temperature depended appreciably on the nominal hydrogen fraction, which is indicative of certain differences in morphology and structure of as-grown samples, including the actual hydrogen content in the phases rich in both rare gases. (Re)crystallization occurred rather quickly, releasing an appreciable amounts of latent heat.

3. Proceeding from the above experimental findings, we think that the states formed in as-grown samples were in many aspects analogs of the helium–impurity media (gels). These mixtures, which comprise two substances differing strongly in molecular parameters and are self-sustained at low temperatures, have a highly amorphous structure and undergo an explosion-like separation at a certain temperature, the value of which depends on the impurity employed.

4. As-grown $Ar–H_2$ condensates exhibited a lesser tendency to form hydrogen–impurity media as compared to Kr-based samples. This finding can also be an indirect confirmation of the assumption made, since the difference in $Kr–H_2$ system is larger than in the $Ar–H_2$ one, by virtue of which the latter system is expected to be less reluctant to form the standard substitutional solid mixtures.

Acknowledgments

This work was supported by the CRDF (grant UP2-2445-KH-02). The authors thank V. V. Khmelenko for communicating results prior to publication and A. A. Solodovnik for valuable discussions.

1. P. Loubeyre, R. LeToullec, and J.P. Pinceaux, *Phys. Rev. Lett.* **72**, 1360 (1994).
2. M.S. Somayazulu, L.W. Finger, R.J. Hemley, and H.K. Mao, *Science* **71**, 1400 (1996).
3. J. Schouten, *J. Phys.: Condensed Matter* **7**, 469 (1995).
4. E.B. Gordon, L.P. Mezhov-Deglin, and O.F.Pugachev, *Pis'ma Zh. Eksp. Teor. Fiz.* **19**, 103 (1974) [*JETP Lett*. **19**, 63 (1974)].
5. E.B. Gordon, V.V. Khmelenko, A.A. Pelmenev, E.A. Popov, and O.F. Pugachev, *Chem. Phys. Lett*. **155**, 301 (1989).

6. R.E. Boltnev, E.B. Gordon, I.N. Krushinskaya, M.V. Martynenko, A.A. Pelmenev, E.A. Popov, V.V. Khmelenko, and A.F. Shestakov, *Fiz. Nizk. Temp* **23**, 753 (1997) [*Low Temp. Phys.* **23**, 567 (1997)].
7. S.I. Kiselev, V.V. Khmelenko, D.M. Lee, V. Kiryukhin, R.E. Boltnev, E.B. Gordon, and B. Keimer, *Phys. Rev.* **B65**, 024517 (2001).
8. S.I. Kiselev, V.V. Khmelenko, D.M. Lee, and C.Y. Lee, *J. Low Temp. Phys.* **128**, 37 (2002).
9. V.V. Khmelenko, S.I. Kiselev, D.M. Lee, and C.Y. Lee, to appear in *Physica Scripta* (2003).
10. V.G. Manzhelii, A.I. Prokhvatilov, I.Ya. Minchina, and L.D. Yantsevich, *Handbook of Binary Solutions of Cryocrystals,* Begell House, New York (1996).
11. I.N. Krupskii, A.I. Prokhvatilov, and G.N. Shcherbakov, *Fiz. Nizk. Temp.* **9,** 83 (1983) [*Sov. J. Low. Temp.* **9**, 42 (1983)]; *Fiz. Nizk. Temp.* **9**, 858 (1983) [*Sov. J. Low. Temp.* **9**, 446 (1983)].
12. A.S. Barylnik, A.I. Prokhvatilov, M.A. Strzhemechny, and G.N. Shcherbakov, *Fiz. Nizk. Temp.* **19**, 625 (1993) [*Low Temp. Phys.* **19**, 447 (1993)].
13. A.S. Barylnik, A.I. Prokhvatilov, and G.N. Shcherbakov, *Fiz. Nizk. Temp.* **21**, 787 (1995) [*Low Temp. Phys.* **21**, 607 (1995)].
14. Ya.S. Umanski, *X-ray Diffractometry of Metals*, Metallurgiya, Moscow (1967) [in Russian].
15. M.A. Strzhemechny, A.I. Prokhvatilov, and L.D. Yantsevich, *Physica* **B198**, 267 (1994).
16. D.L. Losee and R.O. Simmons, *Phys. Rev.* **172**, 944 (1968).
17. P. Loubeyre, R. LeToullec, and J.P. Pinceaux, *Phys. Rev* **B45**, 12844 (1992).
18. S.I. Kiselev, V.V. Khmelenko, E.P. Bernard, and D.M. Lee, *Fiz. Nizk. Temp.* **29**, 678 (2003).